



Quarterly peer-reviewed scientific journal

ISSN 1505-4675
e-ISSN 2083-4527

TECHNICAL SCIENCES

Homepage: www.uwm.edu.pl/techsci/



THERMAL ANALYSIS OF ALUMINUM BRONZE BA1032

Tomasz Chrostek

Department of Materials and Machine Technology
University of Warmia and Mazury in Olsztyn, Poland

Received 8 February 2016, accepted 18 November 2016, available online 21 November 2016.

Key words: thermal analysis, DSC, differential scanning calorimetry, BA1032, $\text{CuAl}_{10}\text{Fe}_3\text{Mn}_2$.

Abstract

In this study, aluminum bronze BA1032 was analyzed thermally by differential scanning calorimetry (DSC). The article presents the results of measurements of phase transitions occurring in aluminum bronze at a temperature of up to 600°C. Thermal analyses were conducted at constant heating rates of 5°C/min, 10°C/min and 15°C/min.

Introduction

Aluminum bronzes increasingly often replace tin bronzes due to their unique properties. Alloys containing up to 11% Al are suitable for industrial applications. Aluminum bronzes with 4–8% Al content can undergo both cold and hot forming, whereas alloys containing 9–11% are used for casting or are hot forged at a temperature of 870°C. Most aluminum bronzes are enriched with Fe and Ni to increase their strength. Aluminum bronzes are characterized by high tensile strength R_m of around 400–600 MPa as well as high corrosion resistance, and they are used in the production of vessel propellers, pump parts, machinery for paper and chemical industries, sheet metal, pipes, gears and wire. Aluminum bronzes with approximately 10% Al content can be hardened due to the presence of eutectoid transformations in the Cu-Al system

Correspondence: Tomasz Chrostek, Katedra Technologii Materiałów i Maszyn, Uniwersytet Warmińsko-Mazurski, ul. Oczapowskiego 11/E27, 10-719 Olsztyn, phone: 89 523 38 55, e-mail: tomasz.chrostek@uwm.edu.pl

at a temperature of 565°C and eutectoid at 11.8% Al. Alloys hardened in water at a temperature of approximately 900°C are tempered at 400–600°C for 2-3 hours. The hardness of quenched CuAl10 is estimated at 180 HB and at around 160 HB after tempering at 500°C (GÓRNY et al. 2003, ROMANKIEWICZ, ROMANKIEWICZ 2007).

Aluminum-iron-manganese bronze BA1032 (CuAl10Fe3Mn2 according to PN-EN 12163:2011) has high corrosion resistance and impact strength. The analyzed alloy is characterized by exceptional resistance to static loading, wear and high temperature, as well as satisfactory fluidity. It is used in the production of machines, engines and parts (rollers, sleeves) exposed to very high mechanical load, corrosion (in particular in acidic solutions) and wear. The BA1032 alloy is also suitable for the production of bars, flats, custom sheet metal and machine parts designed for operation in sea water. The analyzed material has estimated hardness of 120 HB (WIERZBICKA 2000).

Thermal analysis involves a series of methods for determining selected physical properties of a substance across a temperature gradient under a controlled temperature program. Processes that accompany changes in the temperature of various substances are investigated with the involvement thermoanalytical techniques. Differential scanning calorimetry (DSC) is one of such methods, and it is increasingly often used in various areas of science, including in metallurgy. This method is highly useful for measuring phase transition temperature and the amount of heat involved in those processes. Phase transitions structures are already known for the balance of Cu-Al, but there is little information on the phase transformations occurring in aluminum bronze BA1032. Additions of other elements present in the alloy may cause changes in the course of phase transitions (FRĄCZYK, BRECKZO 2010, SECKO, RÓŻAŃSKI 2011, SZUMERA 2012, 2013).

Materials and Methods

Aluminum bronze was tested by dynamic thermal analysis which involves a linear increase and decrease in temperature. The applied method is a fast analytical technique. Analyses were conducted in the DSC Phoenix 204 F1 differential scanning calorimeter (Netzsch) which measures the energy required to establish a zero temperature difference between the analyzed sample and a reference sample. The measured parameter is free heat flow.

Alloy samples weighing 74.92–76.33 mg were placed in aluminum crucibles. Crucibles should have similar weight, and in this experiment, their weight ranged from 39.64 to 40.38 mg. Thermal parameters were measured during heating to a temperature of 600°C at heating rates of 5, 10 and 15°C/min (FRĄCZYK, BRECKZO 2010, SUCHOŃ, JURA 2003).

Results and Discussion

Before the analysis, DSC curves were adjusted with the use of the “DSC Horizontal On” function. This operation was performed to bring the area under the curve where no reactions took place to zero. Adjusted calorimetric curves for BA1032 at heating rates of 5, 10 and 15°C/min are presented in Figure 1.

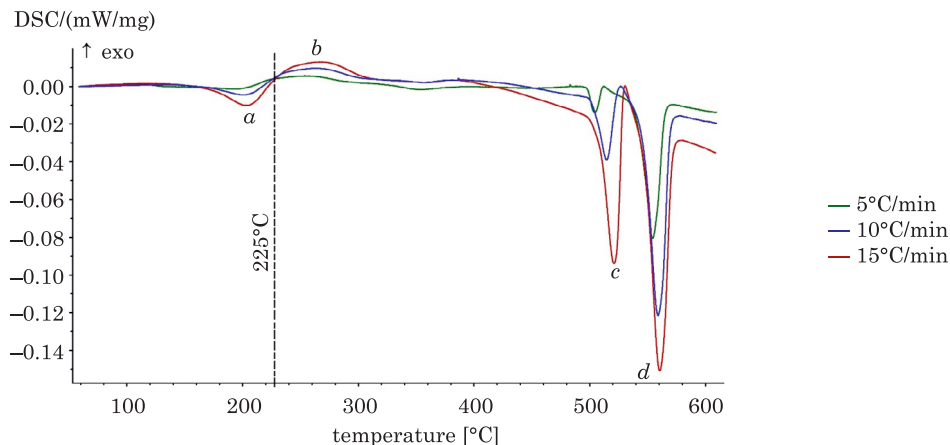


Fig. 1. DSC curves for BA1032 illustrating processes taking place at a temperature of up to 600°C

Information about the exchange of heat between the sample and its environment at different temperatures (T) can be read from a DSC curve. If the DSC curve is a straight (horizontal) line, there are no reactions at a given temperature. Four phase transitions, marked *a*, *b*, *c* and *d*, can be observed in Figure 1 at a temperature of approximately 205°C, 265°C, 515°C and 560°C (peak maxima), for different heating rates.

The first two peaks, *a* and *b*, have low enthalpy which becomes more visible only at a heating rate of 15°C/min. At a temperature of about 205°C reaches the endothermic phase transitions. At a temperature of about 267°C follow on an exothermic phase transition. Figure 2 shows the phase transitions of the peaks *a* and *b* at heating rate 15°C/min.

At a heating rate of 10°C/min and 15°C/min, a minor endothermic effect was noted between peaks *b* and *c* beginning from the temperature of around 390°C.

The last two transitions, *c* and *d*, have well-defined peaks, but their enthalpy is also relatively low. Peaks *c* and *d*, the onset and end of phase transitions, and the enthalpy of each peak at heating rates of 5, 10 and 15°C/min are shown in Figures 3, 4 and 5. Peak maxima denoting the temperatures at which the reaction takes place at the highest rate are also marked.

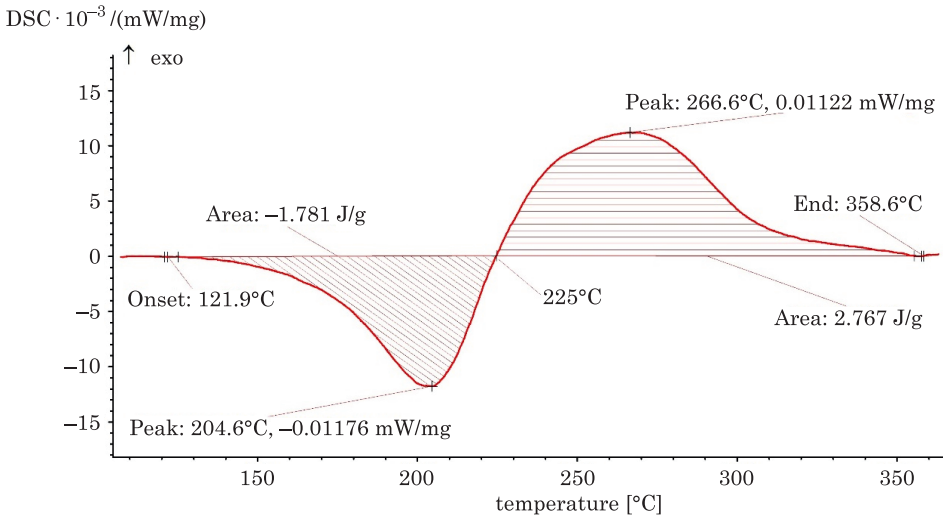


Fig. 2. DSC curves for BA1032 presenting the main reactions taking place at peak *a* and *b* and a heating rate of $15^{\circ}\text{C}/\text{min}$

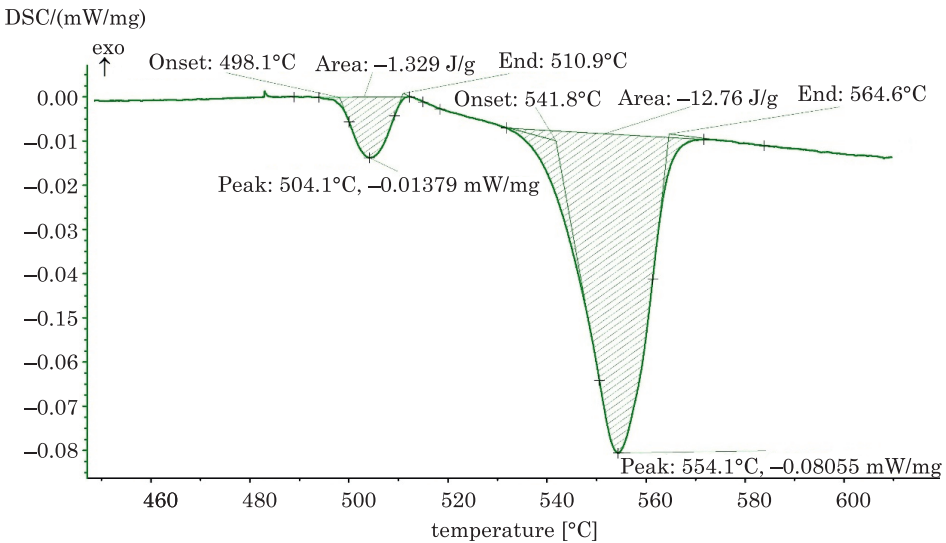


Fig. 3. DSC curves for BA1032 presenting the main reactions taking place at a temperature of up to 600°C and a heating rate of $5^{\circ}\text{C}/\text{min}$

Peaks are more visible at higher heating rates, but peaks positioned close to one another can overlap, which rules out heating at a higher rate. The area under the peak was determined based on the onset and endset values of phase transitions to produce comparable results. Data for peaks *c* and *d* from Figures 3, 4 and 5 are presented in Table 1.

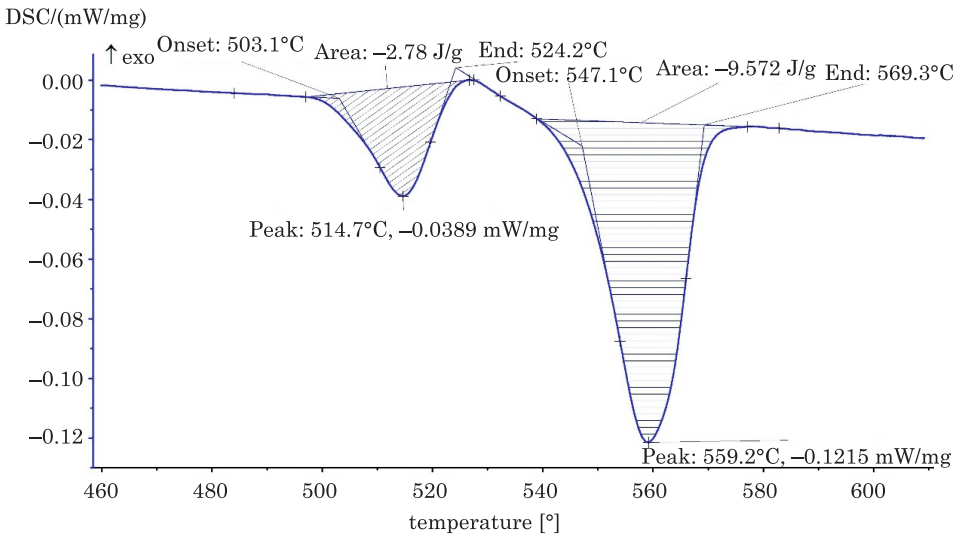


Fig. 4. DSC curves for BA1032 presenting the main reactions taking place at a temperature of up to 600°C and a heating rate of 10°C/min

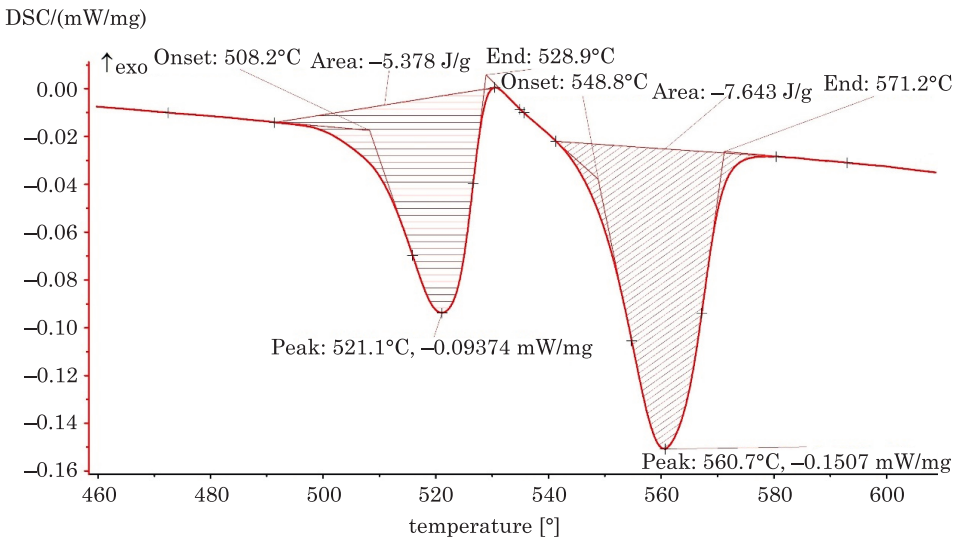


Fig. 5. DSC curves for BA1032 presenting the main reactions taking place at a temperature of up to 600°C and a heating rate of 15°C/min

Table 1
Primary crystallization parameters of BA1032 determined by DSC for peaks *c* and *d*

Heating rate	5°C/min	10°C/min	15°C/min
Peak <i>c</i>			
Onset peak [°C]	498.1	503.1	508.2
Maximum peak temperature [°C]	504.1	514.7	521.1
End peak [°C]	510.9	524.2	528.9
Enthalpy of phase transformation peak [J/g]	-1.329	-2.780	-5.378
Peak <i>d</i>			
Onset peak [°C]	541.8	547.1	548.8
Maximum peak temperature [°C]	554.4	559.2	560.7
End peak [°C]	564.6	569.3	571.2
Enthalpy of phase transformation peak [J/g]	-12.760	-9.572	-7.643

The peaks *c* and *d* create double endothermic effect and it reflects the eutectoid transformation proceeding at temperature of 565°C, in accordance with phase equilibrium diagram Cu-Al. Analogical effect can be observed during the cooling, of the sample: both effects, the solubility limit of phase α and the exothermic effect of eutectoid transformation starting at a temperature of about 538°C and ending at about 473°C, as shown in Figure 6 (GAZDA et al. 2009).

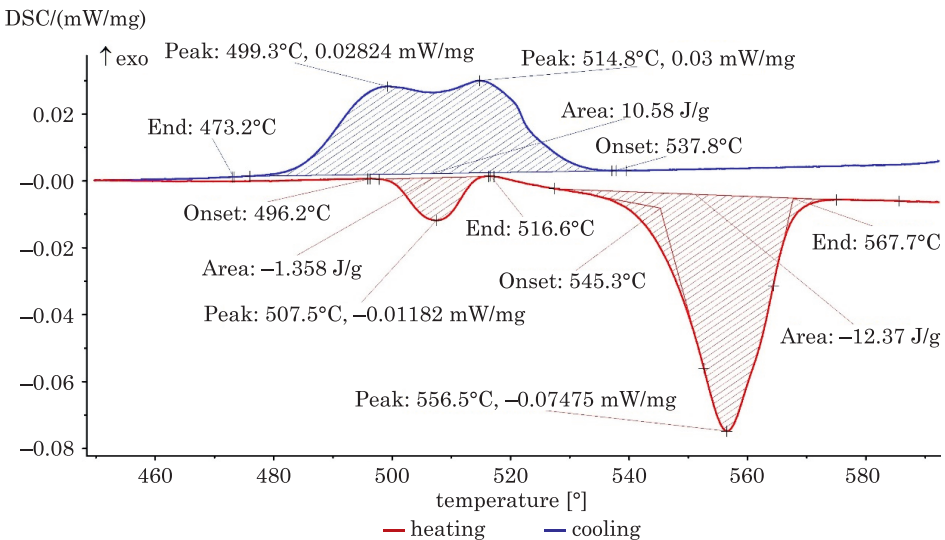


Fig. 6. DSC curves for BA1032 presenting the process of heating and cooling (5°C/min)

Conclusions

Analyzing the results of the research can be concluded that:

– in the present study, four phase transitions were observed in the analyzed material at a temperature of up to 600°C,

– peak broadening can be observed, which indicates that reactions took place relatively slowly within a wide range of temperatures,

– phase transitions *a* and *b* occurred one after the other. An endothermic phase transition ($\nu \rightarrow \alpha + \nu$) took place in peak *a*, whereas an exothermic phase transition ($\alpha + \nu \rightarrow \alpha + \gamma_2$) took place in peak *b*. The temperature of the transition between peaks *a* and *b* was 225°C. The end temperature of peritectoidal transformation ($\alpha + \nu \rightarrow \alpha + \gamma_2$) is 363°C (according to the phase equilibrium diagram), but occurs fastest at a temperature about 267°C. The span across the phase transition is 134°C (od 225°C do 359°C)

– at a heating rate of 10°C/min and 15°C/min, a minor endothermic effect was noted between peaks *b* and *c* beginning from the temperature of around 390°C.

– it confirmed the presence of a double endothermic effect, which consists of peaks *c* and *d*. In peak *c* took place a $\alpha + \gamma_2 \rightarrow \alpha + \gamma_2 + \beta$ transition, whereas in peak *d* a $\alpha + \gamma_2 + \beta \rightarrow \alpha + \beta$ transition. The transitions were noted across a narrow temperature range. The distance between peaks decreased with an increase in heating rate, which can be attributed to an increase in the enthalpy of peak *c* at a higher heating rate. The reverse was observed in peak *d* where enthalpy decreased with an increase in heating rate. When heating rate increases, phase transitions begin later (at higher temperature) and end later, and peak broadening occurs. Energy effects overlap during cooling,

– for industrial practice can be assumed that to achieve the phase $\alpha + \gamma_2$, tempering temperature aluminum-iron-manganese bronze BA1032 should total at least 225°C and not more than 495°C.

References

- FRĄCZYK A., BRECZKO T. 2010. *Study of crystalization of Fe95Si5 amorphous alloy using XRD and DSC*. Materials Physics and Mechanics, 2(9): 85–89.
- GAZDA A., GÓRNY Z., KLUSKA-NAWARECKA S., POLCIK H., WARMUZEK M. 2009. *Comparative studies of the effect of various additives on structure and mechanical properties of CuAl10Fe3Mn2 alloy*. Prace Instytutu Odlewnictwa, 49(1): 5–26.
- GÓRNY Z., KLUSKA-NAWARECKA S., POLCIK H. 2003. *Symulacja krzepnięcia brązu aluminiowego BA1032 z weryfikacją doświadczalną*. Archiwum Odlewnictwa, 3(9): 140–147.
- PN-EN 12163:2011. *Copper and Copper Alloys – Rod for General Purposes*.
- ROMANKIEWICZ F., ROMANKIEWICZ R. 2007. *Study of ferric phase on bronze BA1032*. Archiwum Technologii Maszyn i Automatyzacji, 27(1): 87–91.

- SECKO J., RÓŻAŃSKI P. 2011. *Przykładowe wykorzystanie analizy termicznej w badaniach instytutu metalurgii żelaza*. Instytut Metalurgii Żelaza, Prace IMŻ, 1: 32–39.
- SUCHOŃ J., JURA S. 2003. *Wyznaczenie spektralnego ciepła krystalizacji brązu B102 i BA1032*. Archiwum Odlewnictwa, 3(10): 221–228.
- SZUMERA M. 2012. *Charakterystyka wybranych metod termicznych*. Cz. 1. LAB Laboratoria, Aparatura, Badania, 17(6): 28–34.
- SZUMERA M. 2013. *Charakterystyka wybranych metod termicznych*. Cz. 2. LAB Laboratoria, Aparatura, Badania, 18(1): 24–33.
- WIERZBICA B. 2000. *Obróbka cieplna brązu aluminiowego krzepnącego pod ciśnieniem*. Solidification of Metals and Alloys, 2(42): 117–124.